CrossMark

A net ecosystem carbon budget for snow dominated forested headwater catchments: linking water and carbon fluxes to critical zone carbon storage

Julia Perdrial (iD) **· Paul D. Brooks · Tyson Swetnam · Kathleen A. Lohse · Craig Rasmussen · Marcy Litvak · Adrian A. Harpold · Xavier Zapata-Rios · Patrick Broxton · Bhaskar Mitra · Tom Meixner · Kate Condon · David Huckle · Clare Stielstra · Angélica Vázquez-Ortega · Rebecca Lybrand · Molly Holleran · Caitlin Orem · Jon Pelletier · Jon Chorover**

Abstract Climate-driven changes in carbon (C) cycling of forested ecosystems have the potential to alter long-term C sequestration and the global C balance. Prior studies have shown that C uptake and partitioning in response to hydrologic variation are system specific, suggesting that a comprehensive assessment is required for distinct ecosystems. Many sub-humid montane forest ecosystems in the US are projected to experience increased water limitation over the next decades and existing water-limited forests can be used as a model for how changes in the hydrologic cycle will impact such ecosystems more broadly. Toward that goal we monitored precipitation, net ecosystem exchange and lateral soil and stream C fluxes in three semi-arid to sub-humid montane forest catchments for several years (WY 2009–2013) to investigate how the amount and timing of water delivery affect C stores and fluxes. The key control on aqueous and gaseous C fluxes was the distribution of water between winter and summer precipitation, affecting ecosystem C uptake versus heterotrophic respiration. We furthermore assessed C stores in soil and above- and belowground biomass to assess how spatial patterns in water availability influence C stores. Topographically-

Responsible Editor: Marc G. Kramer.

J. Perdrial (✉)
Department of Geology, University of Vermont,
Burlington, VT, USA
e-mail: jperdria@uvm.edu

J. Perdrial · C. Rasmussen · A. Vázquez-Ortega ·
R. Lybrand · M. Holleran · J. Chorover
Department of Soil, Water and Environmental Science,
University of Arizona, Tucson, AZ, USA

P. D. Brooks · X. Zapata-Rios · P. Broxton ·
T. Meixner · K. Condon · D. Huckle · C. Stielstra
Department of Hydrology and Atmospheric Sciences,
University of Arizona, Tucson, AZ, USA

T. Swetnam · B. Mitra
School of Natural Resources and Environment, University
of Arizona, Tucson, AZ, USA

K. A. Lohse · M. Litvak
Department of Biological Sciences, Idaho State
University, Pocatello, ID, USA

M. Litvak
Department of Biological Sciences, University of New
Mexico, Albuquerque, NM, USA

C. Orem · J. Pelletier
Department of Geosciences, University of Arizona,
Tucson, AZ, USA

Springer

driven patterns in catchment wetness correlated with modeled soil C stores, reflecting both long-term trends in local C uptake as well as lateral redistribution of C leached from upslope organic soil horizons to convergent landscape positions. The results suggest that changes in the seasonality of precipitation from winter snow to summer rain will influence both the amount and the spatial distribution of soil C stores.

Introduction

Carbon (C) storage in terrestrial ecosystems has an important function in regulating global climate and is therefore intensively studied (Bloom et al. 2016; Houghton 2005; Houghton et al. 1998; Lal 2005; Schimel et al. 2001). The C balance of terrestrial systems varies both regionally and by ecosystem type (Bradford and Crowther 2013; Houghton 2007; Houghton et al. 1998) but aggrading forested systems typically act as net C sinks on the time scale of decades as biomass accumulates (Amiro et al. 2010; Lal 2005; Schimel et al. 2001) and centuries as C is transferred to soil (Kaiser et al. 1996; Lal 2004; Schmidt et al. 2011). The amount of C exchanged among atmospheric, terrestrial and aquatic reservoirs depends on a complex interplay between various drivers such as climate, topography (Lybrand and Rasmussen 2015), parent material (Heckman et al. 2009), substrate age (Torn et al. 1997), land use, and biota. Quantifying these reserves and exchanges is a fundamental step towards predicting future C source/sink dynamics.

Several studies have compiled partial budgets, for example, by quantifying riverine C efflux and stream water exchange and comparing these with atmospheric fluxes (Jonsson et al. 2007; Öquist et al. 2014; Rowson et al. 2010; Shibata et al. 2005; Zhou et al. 2013). A recent study by Öquist et al. (2014) showed decreased annual net C uptake in a seasonally snow covered boreal catchment during wet years because associated cloud cover induced energy limitation of vegetation productivity. The decrease in net uptake was accompanied by increased lateral aqueous C losses, potentially diminishing the capacity of the boreal forest critical zone (CZ) to act as a C sink in wet years. These results highlight the complex and unanticipated interactions between ecosystem C uptake and lateral losses that can occur with inter-annual variation in climate. Questions remain as to whether these types of patterns hold true across other seasonally snow covered environments. While several studies have examined gross primary productivity (GPP) as a driver of biomass accretion (Keith et al. 2009) and soil C stabilization (Battin et al. 2009; Lal 2005; Schimel et al. 2001), other components of the systems remained unmeasured in these studies. Full C budgets—i.e., the inventory of C fluxes and stores that would allow for additional insight into the rate of accretion to or loss from various stores—have not been compiled at the watershed scale.

Seasonally snow covered ecosystems are particularly important because they are abundant (covering one-third of the Earth's land surface) and sensitive to climate change. Changes in the climate system will lead to an overall redistribution of precipitation (IPCC 2013) and alter the partitioning of C uptake and loss. A markedly vulnerable subgroup of seasonally snow-covered environments is represented by semi-arid and sub-humid ecosystems where the amount and timing of water delivery may limit net primary productivity. Impacts of climate change, such as a decline in winter snow and mean annual precipitation (MAP), and increases in mean annual temperature (MAT) and vapor pressure deficit (VPD), are expected to manifest themselves sooner in these systems (Breshears et al. 2008; Park Williams et al. 2013). Even small shifts in the timing or spatial distribution of water delivery may impact C dynamics in fundamental ways.

The principal C fixers in forested systems are deeply-rooted autotrophs with access to ground water (Gochis et al. 2010). Furthermore, recent work has

P. D. Brooks
Department of Geology and Geophysics, University of Utah, Salt Lake City, UT, USA

A. A. Harpold
Department of Natural Resources and Environmental Science, University of Nevada, Reno, NV, USA

R. Lybrand
Department of Crop and Soil Science, Oregon State University, Corvallis, OR, USA

A. Vázquez-Ortega
School of Earth, Environment and Society, Bowling Green State University, Bowling Green, OH, USA

suggested that lateral ground water subsidy can supplement plant available water, increasing forest C uptake in areas of topographic convergence (Fan et al. 2013; Thompson et al. 2011a, b). In snow-dominated systems, this ground water is typically recharged during snowmelt (Zapata-Rios et al. 2015b) and is utilized in the following growing season. In contrast, soil microorganisms contributing to heterotrophic soil respiration, do not have access to this deep water supply, but are instead dependent on summer rains to support their metabolism. These biological demands for water thereby limit its availability for aqueous lateral C transfers as well as for vertical heterotrophic respiratory fluxes. Together, these catchment-scale hydrological processes suggest that differences in the seasonality of precipitation influence both temporal and spatial patterns in C storage and flux.

We therefore postulate (hypothesis 1) that GPP is highest in years with wet winters and that ecosystem respiration (R) is greatest in years with wet summers, resulting in smallest net ecosystem C uptake in years with dry winters and wet summers. We further hypothesize that—unlike wetter sites, such as the boreal forest sites studied by Öquist et al. (2014)—in sub-humid forests, soil and stream water dissolved C fluxes are small relative to land–atmosphere exchange because water is either partitioned into groundwater stores and/or consumed in evapotranspiration (hypothesis 2). Furthermore, if C fluxes depend on water availability, long term trends in wetness might be reflected in C stores as well. We therefore hypothesize that catchments with greatest wetness will exhibit largest biomass and soil C stores (hypothesis 3).

In order to investigate the links between inter-annual variation in climate, precipitation timing, and C fluxes and stores for such a snow-dominated system, we compiled a complete C budget for three headwater catchments in the Jemez River Basin Critical Zone Observatory (JRB-CZO). The semi-arid to sub-humid climate of our study site includes high inter-annual precipitation variability, with approximately half of the annual precipitation introduced as snow and the other half as summer (monsoon) rain. Specifically, we: (i) monitored biosphere–atmosphere exchange of water and C with eddy covariance estimates of net ecosystem exchange (NEE), GPP, and ecosystem respiration; (ii) quantified soil C fluxes, and (iii) measured lateral C exports in streamflow in all three catchments for water years (WY) 2009–2013. We furthermore assessed C storage in soil and biomass as well as shallow groundwater.

Materials and methods

A summary of data acquisition methods is presented here with more details provided in the electronic online resources.

Site description

The three headwater catchment ecosystems reside on different aspects of a single resurgent rhyolitic dome, Redondo Peak, in the Jemez River Basin Critical Zone Observatory (JRB-CZO), located in the Valles Caldera National Preserve (VCNP) northwest of Albuquerque, NM at 35.8°N, 106.5°W (Fig. 1a, b). The catchments drain the north, east and southeast slopes of Redondo, allowing us to explore several catchments of similar physiographic characteristics, including drainage area, bedrock type, regional climate, vegetation, slopes and elevation gradients (Table 1) (Perdrial et al. 2014a). Vegetation in all three catchments is dominated by mixed-conifer species including blue spruce (*Picea pungens*), Douglas fir (*Pseudotsuga menziesii*), white fir (*Abies concolor*), corkbark fir (*A. lasiocarpa var. arizonica*), Engelmann spruce (*Picea engelmannii*) and some interspersed aspen (*Populus tremuloides*) (Broxton et al. 2009; Coop and Givnish 2007; Muldavin and Tonne 2003). Soils on Redondo include a mix of Mollisols, Andisols, Alfisols, and Inceptisols (Fig. 1c, Muldavin and Tonne (2003)). All soils classify as "Vitrandic" subgroup (SoilSurveyStaff 2011) and are characterized by an abundance of volcanic glass, moderate to strong acidity, clay contents ranging from 15 to 39%, and organic C contents ranging from 29% in some surface horizons to less than 0.2% in subsoils (Vazquez-Ortega 2013). Inorganic C was not detected in these soils. Secondary mineral phases include kaolinite and smectitic clays, and smaller mass fractions of crystalline and short-range-order (oxyhydr)oxides (Vazquez-Ortega 2013; Vázquez-Ortega et al. 2015).

The dominantly north-facing catchment, Jaramillo Creek, hereafter denoted 'N', drains an area of 305 ha, whereas La Jara is dominantly east-facing (hereafter denoted 'E', 367 ha) and History Grove is south-east-facing (hereafter denoted 'SE', 242 ha, Fig. 1b). All
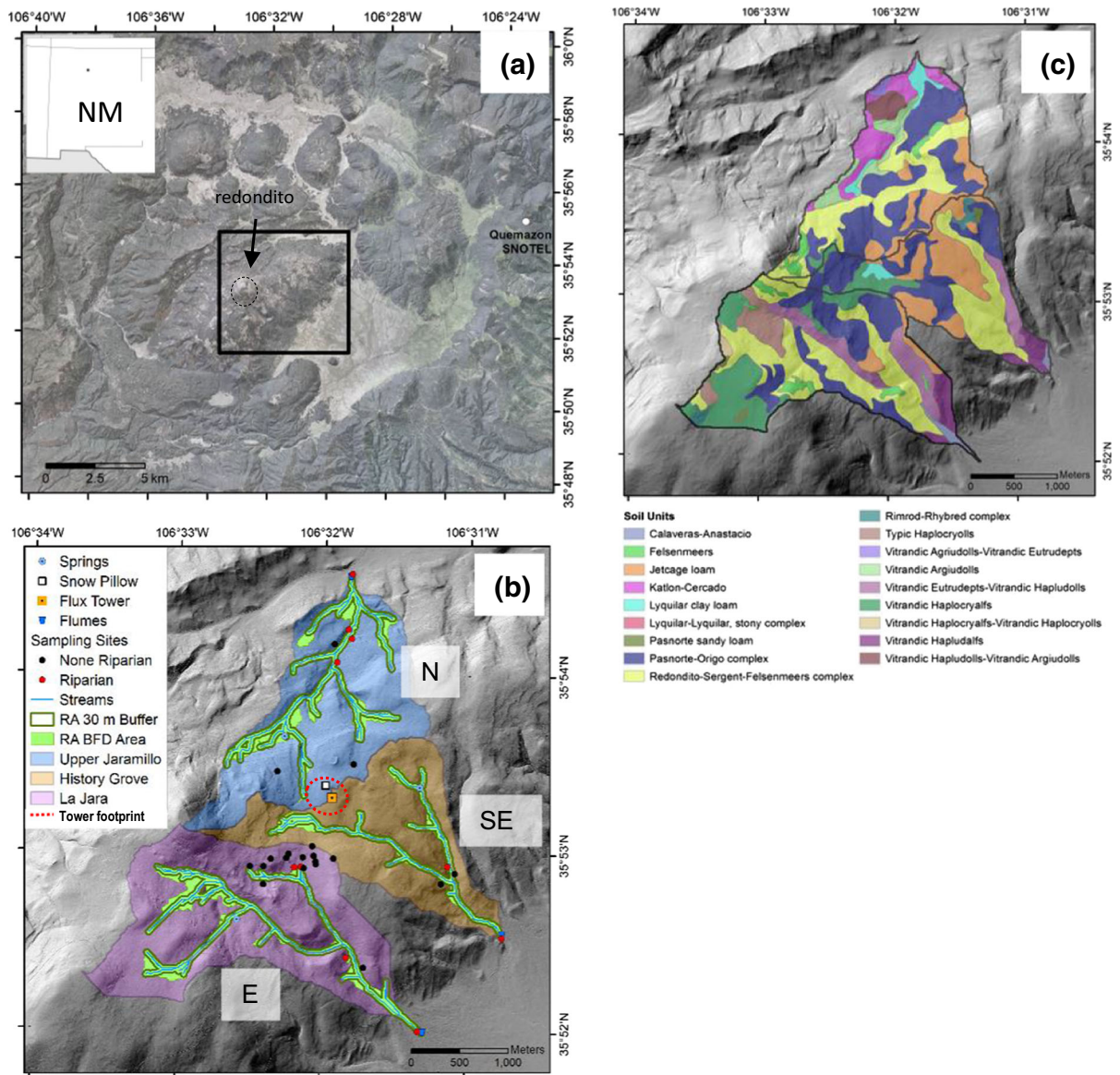
Fig. 1 **a** Location of Redondo dome within the Valles Caldera National Preserve (VCNP) in northern New Mexico. **b** Jemez River Basin Critical Zone Observatory (JRB-CZO) catchments around Redondo Dome showing riparian area contribution and plot location delineated based on a 1 m digital elevation map. **c** Dominant soil units of study catchments

Table 1 Characteristics of studied catchments. Aspect (in degrees) of 360 is north, 90 is east, and 180 south

Catchment	Aspect (degrees)	Area (ha)	Elevation (m) min < mean ± SD < max	Slope % ± SD	Canopy cover > 2 m agl (%)	% Riparian
N	353	305	2.722 < 2.925 ± 117 < 3.323	27 ± 19	48.77	18 ± 0.3
SE	113	242	2.862 < 2.948 ± 96 < 3.308	24 ± 13	55.52	13 ± 1.6
E	95	367	2.701 < 3.100 ± 155 < 3.429	29 ± 17	59.86	15 ± 0.3

catchments were logged in the 1930s–1970s (Allen 1989), however N was logged more intensively (Parmentier et al. 2007). Topographic characteristics (e.g., slope, aspect, drainage area, and local curvature) were calculated from a 1 m resolution bare-earth digital elevation model (DEM) derived from a light detection and ranging (LiDAR) dataset collected by the National Center for Airborne Laser Mapping (NCALM) in summer of 2010 (ArcGIS10.0, data available at http://criticalzone.org/catalina-jemez/data/). Topographic wetness index (Beven and Kirkby 1979) was calculated as $\lambda = \ln(a/\tan\beta)$, where a is the unit or specific catchment area in meters (calculated here using the D-inf multiple-flow-direction algorithm for flow routing (Tarboton et al. 1991), and β is the slope in degrees, based on the DEM. Solar radiation was computed on a monthly basis using an hourly time step, a sky view of 300 pixels, 32 calculation directions, eight zenith and azimuth divisions, and uniform clear sky conditions using ArcGIS Spatial Analyst Tools (Fu and Rich 1999). Effective energy and mass transfer (EEMT)—a measure of the energy available for weathering below the ground surface as derived from both effective precipitation and net primary production (Rasmussen et al. 2011)—was calculated according to the $EEMT_{TOPO}$ method described in Rasmussen et al. (2015), which includes contributions from lateral water transport and aspect-induced variation in vegetation productivity.

Climate and hydrologic response

Over the study period mean annual temperature in the JRB-CZO catchments ranged from 4.2 to 5.3 °C, with large variations in minimum—but not maximum—values (Table 2). Precipitation was bimodal; approximately half of mean annual precipitation is snow during winter (October–April) and the other half is rain during the North American Monsoon (July–September). Total precipitation varies from about 550 mm at 2600 m a.s.l to 830 mm at 3000 m a.s.l, with increases at higher elevation due to local orographic lifting (Brooks and Vivoni 2008). Stream discharge during spring snowmelt is ca. an order of magnitude higher than winter base flow, although discharged water derives from pressure-wave induced displacement of ground water that has a subsurface residence time of > 1 years (Zapata-Rios et al. 2015b). Conversely, due to greater evapotranspiration demand in summer, North American Monsoon rains result in less stream water yield than does snowmelt (Broxton et al. 2009; Liu et al. 2008).

Distributed water balance with SnowPALM

We used SnowPALM, a high temporal (1 h) and spatial (to 1 m) resolution mass and energy balance microclimate model, to distribute measurements of rainfall, snowmelt, and evapotranspiration for each of the study catchments (Broxton et al. 2015). SnowPALM accounts for topographic and vegetation influences on radiation, interception, and the turbulent exchanges of mass and energy at the snow surface by combining a variety of existing formulations for processes such as interception (Pomeroy et al. 1998), canopy attenuation of radiation (Mahat and Tarboton 2012) and wind distribution of snowfall (Winstral et al. 2002), on top of an energy balance snow model (online resource).

Carbon budget

We combined direct observations of land–atmosphere exchange, soil solution flux, and hydrologic export in stream water with spatially extensive observations of storage in biomass and soil to evaluate controls on long-term C storage in catchment ecosystems.

Annual C uptake

NEE and GPP data were obtained from an eddy covariance flux tower situated in mixed conifer forest

Table 2 Mean annual and seasonal temperatures for the study sites for 4 years derived from the weather station of the Zero Order Basin in E (http://criticalzone.org/catalina-jemez/data)

Water year	2009	2010	2011	2012
Mean annual temperature (°C)				
Average	4.7	4.2	5.1	5.3
Min	− 16.2	− 15.3	− 26	− 11.7
Max	19.1	19.0	19.3	18.1
Seasonal temperature (°C)				
Average winter	− 0.5	− 1.7	− 0.3	0.1
Average summer	11.9	12.4	12.5	13.1

on a ridge between the N and SE catchments. The tower is part of both the JRB CZO and the AmeriFlux network (Valles Caldera Mixed Conifer/US Vcm, http://ameriflux.ornl.gov (Anderson-Teixeira et al. 2011; Perdrial et al. 2014a), Fig. 1b). Tower-based NEE values were partitioned into total C uptake through photosynthesis (GPP) and total ecosystem respiration (Ciais et al. 2005). We note that respiration may be underestimated (NEE and GPP overestimated) due to the position of the tower on the ridge top (Pypker et al. 2007). We subsequently partitioned annual C inputs into above and below ground allocations using the relationships between productivity and total below ground C allocation developed by Litton et al. (2007). Herbaceous productivity was quantified in 41 grassland monitoring transects through differential clip harvests in the spring and fall and checked against results from clip harvests in 32 one m^2 plots sampled on two 80 m transects at the flux tower in the spring and fall. Every 10 m, two plots were harvested, one under the forest canopy, and one in the interspace (online resource).

Hydrologic C export

Soil dissolved organic carbon (DOC) and water fluxes were measured during 2011 and 2012 using 18 passive capillary wick samplers (PCAPS, Perdrial et al. 2012) installed in the headwaters of E. DOC flux was calculated as (DOC concentration * volume collected)/PCAP sampler area. Because the wicks release dissolved inorganic carbon (DIC), PCAPS are not recommended for the quantification of DIC fluxes (Perdrial et al. 2014b). For DIC flux calculations, we used results from co-located suction cup samplers (Prenart, Superquartz^{TM}, Denmark), since these do not introduce chemical artifacts. Based on these samples, we established a rating curve to calculate [DIC] = $-$2.565*Ln[DOC] + 11.12. DIC flux was then calculated as for DOC flux, using water volumes collected by the PCAPS cross-sectional area (online resource).

We quantified C leached from O-horizons using the significant correlation between soil water and DOC fluxes obtained from the PCAPS in E. No overland flow was observed in these catchments suggesting that all rainfall or snowmelt infiltrates into at least the shallow soil layers and that hence total precipitation is a proxy for shallow soil water flux (Liu et al. 2008; Zapata-Rios et al. 2015a). To estimate this flux for

each catchment we used the SnowPALM output for total precipitation for each catchment and calculated water flux using the correlation established for E. Subtracting ground and stream water fluxes from the soil infiltration flux yields an estimate of soil water C that is transferred laterally to convergent landscape positions.

Stream water grab samples were collected at midday 10 times during WY 2010, 20 times during WY 2011 and 19 times during WY 2012 from March (pre-snowmelt) to October (post-North American Monsoon). No stream water was sampled over the winter due to access limitations, but hydrograph data indicate consistent base flow discharge values prior to the snowmelt sampling period. Analysis of DIC involved instrumental acidification of solution followed by purging for infrared measurement of CO_2, whereas analysis of DOC was by high temperature combustion of the purged samples, followed also by infrared CO_2 detection (Shimadzu TOC-VCSH, Columbia, MD, USA).

Daily discharge data, obtained from pressure transducer recordings from flumes with established rating curves, and solute concentrations were used to calculate volume weighted mean concentrations (VWM) for streams (Vázquez-Ortega et al. 2015). Uncertainty in stream water C flux was calculated on the basis of a combined maximum analytical error of 5% and a discharge measurement error of 10% (Perdrial et al. 2014a, b). Sampling bias (particularly important during winter months) was included using a Tukey's jackknife variance estimation (Efron and Stein 1981).

Spatially distributed C stores

Biomass C

We combined airborne LiDAR mapping, intensive forest inventory plots, and biomass harvest to quantify the spatial distribution of biomass C storage. In summer of 2010, our team measured above-ground biomass (AGB) in 48 radial 0.1 ha inventory plots distributed randomly across the JRB-CZO as part of a LiDAR vegetation biomass calibration effort (Swetnam 2013). Aerial LiDAR was collected in June 2010 by the National Center for Airborne Laser Mapping (NCALM) with an Optech Gemini (Optech Inc.

Vaughan, ON) using four returns per pulse, operated 1000 m above ground level.

Average herbaceous aboveground C measurements (Mg C ha^{-1}) for the study period were distributed spatially using mapped montane grasslands, grazeable forest/woodland, and mesic (i.e. riparian) meadows (Muldavin et al. 2006). Below ground herbaceous C and woody C were estimated from below-to-above ground ratios [online resource, also referred to as root-to-shoot ratios (Jackson et al. 1996)] derived from other studies of the same or similar vegetation types (Cairns et al. 1997; Santantonio and Hermann 1985; Whittaker and Niering 1975). Below ground biomass (BGB) was estimated as 33% of above ground biomass (Robinson 2004). Tables are provided in the online resource.

Soil and litter C

Surface detritus (also referred to as 'necromass'), including the down woody debris and duff layer, i.e., O-horizon, was measured using the line-intersect method (Brown 1971). Soil C concentrations were determined for a total of 61 soil horizons throughout the study area (locations indicated in Fig. 1b). Sampling was designed to capture both organic and mineral horizon depth, bulk density, and organic C content across a range of landscapes. Twelve locations were extensively sampled and characterized in 2010 across a range of landscape (variable aspect, planar, divergent and convergent) positions down to the depth of refusal (ranging from 84 to 125 cm depth) in E (SoilSurveyStaff 2011). Because most C was found in the top 20 cm, additional surface soil samples down to ca. 20 cm were collected from 17 locations from catchment SE and N. Total soil C stocks presented here represent the sum of organic and mineral horizon contributions. Error propagation, based on standard deviations of mineral and organic horizon C concentrations, was used to constrain the error on total soil C stock estimates (online resource).

Soil C mass fraction was determined on the fine earth (< 2 mm) fraction of all samples using high temperature dry combustion with CO_2 quantification by infrared gas analysis on a Shimadzu TOC-VCSH analyzer equipped with SSM-5000A solid sample module (Columbia, MD, USA). Inorganic C was measured using the same instrument operated at lower temperature to assess CO_2 evolution upon H_3PO_4 addition, but inorganic C was below detection limit in all soil samples.

Soil C data from discrete sampling locations were used to generate a landscape scale model soil C stocks throughout the three catchments, building on observed differences among riparian and hillslope landscape locations. Soil pit data collected as described above, as well as 160 soil profile descriptions collected previously (USFS, unpublished) indicated that nearly all soil profiles exhibited an exponential decrease in C content with depth (online resource). An exponential model fit to all available soil profiles effectively described the C decrease with depth. A generalized exponential model using the median parameter estimates coupled with modeled soil depth following Pelletier and Rasmussen (2009) was used to extrapolate soil C stocks (online resource).

Shallow ground water

Ground water from springs and seeps were sampled in all three catchments in spring and summer of WY2012 (Fig. 1b). Previous research indicated that residence times are consistent with snowmelt recharge and use by vegetation the following year (Broxton et al. 2009). Samples were processed and analyzed as described for stream water samples below. DIC and DOC masses in ground water were then calculated by multiplying spring water C concentrations, averaged over each year for each catchment, by ground water storage volume as calculated by Zapata-Rios et al. (2012) for the years 2010 and 2011 (online resources).

Statistical analyses

All statistical analyses were performed using JMP pro 11 (SAS, Cary, NC). Data used for correlations and analysis of variance (ANOVA) were tested for normality by evaluating the goodness of fit (Shapiro-Wilkes) to normal distributions. Values below Prob < W of 0.05 indicate non-normality of the underlying distribution. For all data, Prob < W values were above this threshold (0.9 and higher) with the exception of snow water equivalent (in SE), effective precipitation and total summer precipitation (in E). However, even in these cases, Prob < W values were very close to the threshold (0.04) and normal distribution is likely. Repeated measures ANOVA was performed to test for

main effect of year, catchment, or a combination of both.

Results

Inter-annual variation in hydroclimate

Both point observations and the SnowPALM model results for distributed precipitation showed high variations in inter-annual precipitation (Table 3). Total precipitation was similar for the three catchments, decreasing over the course of 4 years. Maximum snow water equivalent (SWE) was similar for the WYs 2009, 2010 and 2012, but SWE for WY2011 was significantly lower ($p < 0.0001$). Summer precipitation was highest following the dry winter in WY2011 and lowest in WY2012 ($p < 0.02$). Effective precipitation (i.e., total precipitation minus evapotranspiration) was typically positive in winter, when precipitation exceeded evapotranspiration, and negative in summer, when evapotranspiration outpaced seasonal precipitation. The exception was the wet summer of WY2011 when, due to a combination of increased precipitation and reduced evapotranspiration, effective precipitation for the catchments ranged from 47 to 80 mm versus -74 to 5 mm for the other years. Comparing the distribution of precipitation among the three catchments, SE appears the driest in all years for both winter and annual effective precipitation, whereas E was often the wettest catchment, but due to large inter-annual variability these differences were not significant when data are integrated over the full study period (prop $>$ F > 0.4).

Spatial variation of radiation, wetness and EEMT

Radiation and EEMT varied amongst catchments while wetness varied by landscape position. E and SE received more solar radiation, mostly at higher elevation, than N (Fig. 2a). Annual catchment averages for solar radiation in GJ ha^{-1} were 61,760 for N, 68,340 for SE and 67,910 for E. Topographic wetness varied with landscape position in each catchment but the catchments exhibited similar average values because of similar slope (ranging from 8.7 for N to 8.8 for E, Fig. 2b). EEMT was highest in E and N, mostly at higher elevation due to increased solar radiation and precipitation (Fig. 2c).

Gaseous C fluxes: catchment-scale GPP, ecosystem respiration and NEE

Gross primary productivity showed large inter-annual variability; it was highest in WY2012 and lowest in the dry WY2011. Due to relatively high respiratory C losses, WY2011 showed the least negative NEE values (25% lower magnitude NEE compared to the wetter years; the negative values indicating net ecosystem C uptake). For the other years, respiration was similar (ranging from 6.50 to 6.79 Mg C ha^{-1} year^{-1}) but variations in GPP resulted in variable NEE (Table 4).

Aqueous C fluxes

Stream water DOC and DIC exports were three orders of magnitudes lower than observed NEE (Table 4), but similarly impacted by inter-annual variability in

Table 3 SnowPALM results of precipitation in mm for all 3 catchments

Water year	2009			2010			2011			2012		
Catchments	N	SE	E	N	SE	E	N	SE	E	N	SE	E
P_{tot}	747	752	778	683	677	740	650	659	663	588	595	494
SWE_{max}	211	188	210	221	196	250	94	79	104	238	207	254
Psummer	306	305	306	282	281	294	330	333	299	220	231	90
P_{eff}	224	191	241	196	164	239	138	112	142	166	127	144
P_{eff} summer	-1	-8	0.1	0.3	-2	5	79	80	47	-26	-37	-74

Total precipitation (P_{tot}), maximum snow water equivalent (SWE_{max}), summer precipitation (Psummer), effective precipitation for the entire year (P_{eff}) and the summer months (06/01–09/30, P_{eff} summer). Associated error for model output is estimated to be 14%, a value that is derived from the comparison of model output and actual measurements (Broxton et al. 2015)
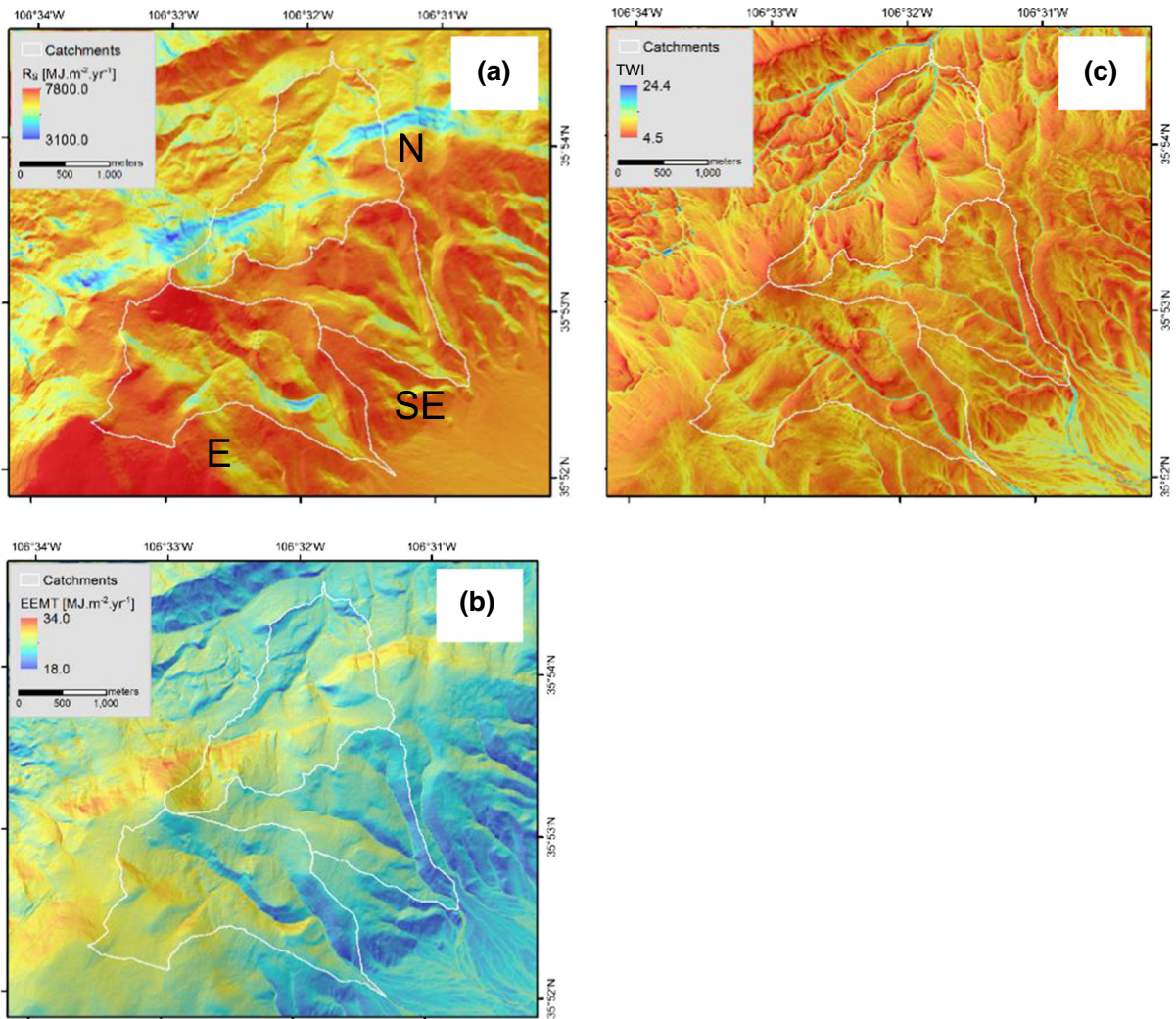
Fig. 2 Maps derived from 1 m resolution bare earth LiDAR DEM for **a** solar radiation, **b** topographic wetness index (TWI), and **c** for effective energy and mass transfer (EEMT)

precipitation. Stream water C fluxes were lowest for the dry WY2011, significantly higher for WY2010 ($p < 0.02$) and intermediate for WY2012. Compared to the two other catchments, N exported more DOC (33–57%) and DIC (30–67%) in stream water across all WY's (Table 4). Total riverine C effluxes accounted for less than 0.25% of NEE, with the lowest riverine contribution in the dry WY2011.

Dissolved soil C fluxes

Total dissolved soil C fluxes (DOC + DIC) measured at different locations within a headwater zero-order catchment were variable but, averaged over 3 years,

they were four times higher than the average riverine C export suggesting that large amounts of soil C were being redistributed within the catchment along sub-surface flowpaths. Dissolved soil C fluxes again varied with inter-annual variation in precipitation during WY 2011–2013 (Fig. 3). The highest soil C fluxes were observed in the O-horizons across all years with WY2012 producing larger fluxes in the near surface horizons. The difference in fluxes between years was only significant for the O horizon (student test, $p < 0.03$), and close to the threshold for B/C horizon for 2011 versus 2013 ($p < 0.07$). Mineral soil horizons yielded significantly less soluble C flux than the O-horizons (student test, $p < 0.03$).

Table 4 Carbon fluxes for the study area and WY2009–2012 in Mg ha^{-1} year^{-1} from the flux tower for gross primary productivity (GPP), ecosystem respiration (R), and net ecosystem exchange (NEE) and in kg ha^{-1} year^{-1} for dissolved organic and inorganic stream water fluxes (DOC and DIC, all reported as C)

	2009			2010			2011			2012		
gaseous fluxes [Mg ha^{-1}yr^{-1}]												
GPP	11.67			12.86			11.52			13.44		
R	6.50			6.64			7.44			6.79		
NEE	-5.17			-6.22			-4.08			-6.65		
riverine effluxes [kg ha^{-1}yr^{-1}]												
		N	SE	E	N	SE	E	N	SE	E		
DOC	NA	6.85	4.56	3.39	2.08	1.25	1.13	5.43	2.84	2.35		
stdev	NA	0.16	0.12	0.06	0.05	0.00	0.01	0.09	0.04	0.04		
DIC	NA	8.94	5.49	6.25	2.73	0.91	1.57	4.57	2.51	2.81		
stdev	NA	0.39	0.13	0.18	0.09	0.00	0.03	0.05	0.05	0.03		
Total riverine fluxes	NA	15.79	10.05	9.64	4.81	2.16	2.7	10	5.35	5.16		
Std Err	NA	0.42	0.18	0.19	0.10	0.00	0.03	0.10	0.06	0.05		

Connecting water and C fluxes

The impact of seasonality of precipitation on C fluxes is exemplified by the strong, significant correlations of water versus gaseous and aqueous C fluxes (Fig. 4). Annual respiration showed a positive correlation with effective summer precipitation (Fig. 4a) while GPP and NEE were negatively correlated with total and effective summer precipitation ($r^2 = 0.57$ and 0.54 for GPP and 0.47 and 0.76 for NEE, respectively, $p < 0.005$, data not shown). The relationship of annual NEE with winter precipitation showed the opposite trend, where an increase in maximum snow water equivalent (SWE) led to an increase in net ecosystem C uptake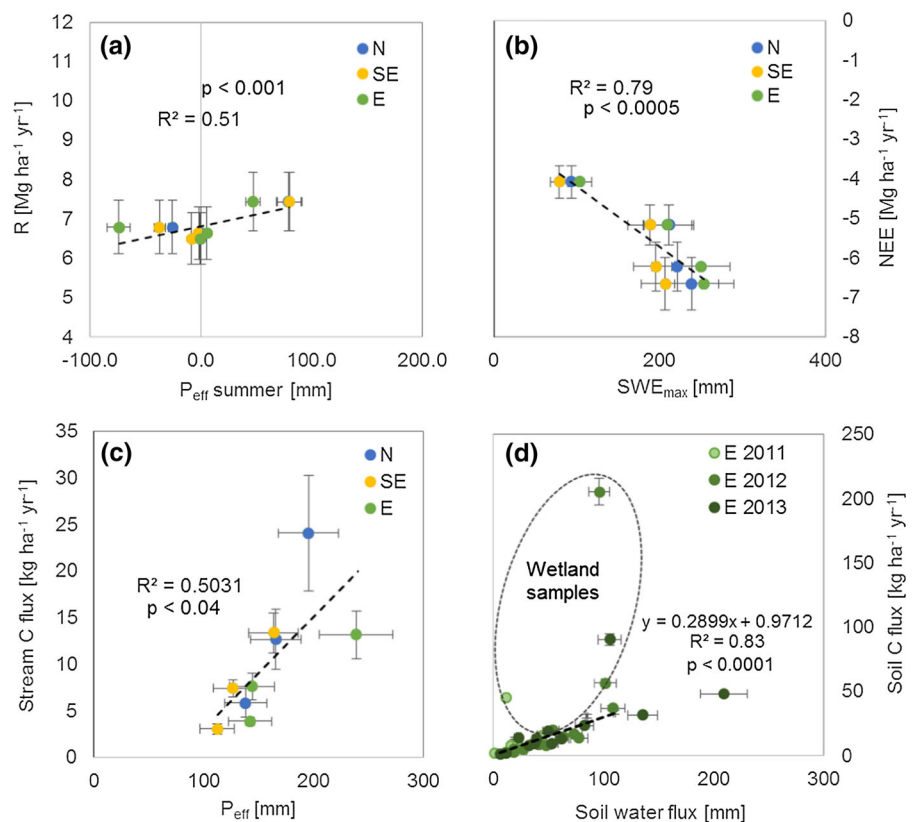 (negative NEE, Fig. 4b). This relationship was mostly driven by increased GPP in snow rich years ($r^2 = 0.72$, $p < 0.009$, data not shown). Stream water C fluxes showed a significant positive correlation with annual effective precipitation (Fig. 4c) and weaker correlations with SWE ($r^2 = 0.39$, $p = 0.07$) and effective summer precipitation ($r^2 = 0.13$, $p > 0.3$, data not shown). Soil dissolved C fluxes correlated significantly with soil water fluxes (Fig. 4d). Very high soil C fluxes for relatively low water fluxes were measured in samples derived from one wetland-type location in the catchment. Comparing monthly total precipitation with GPP, ecosystem respiration, NEE and soil C fluxes shows the pronounced seasonality of water and C fluxes (also see online resources). Total water input to the systems was
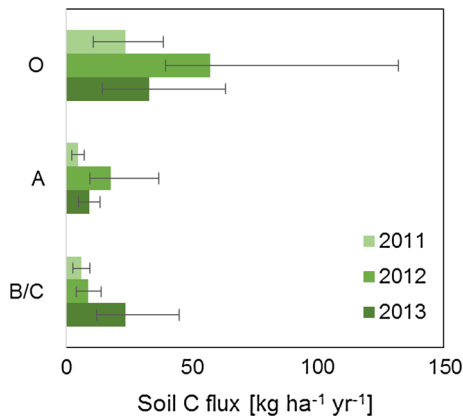
Fig. 3 Soil dissolved C (DOC and DIC) fluxes as a function of approximate genetic soil horizon averaged over 6 soil pit locations in the E headwaters for WY2011–2013. *O* organic horizon, *A* accumulation horizon, *B/C* mineral soil close to bedrock

high during snowmelt and the growing season and led to high GPP, high respiration, high negative NEE (since GPP > respiration) and lateral fluxes (soil and stream water).
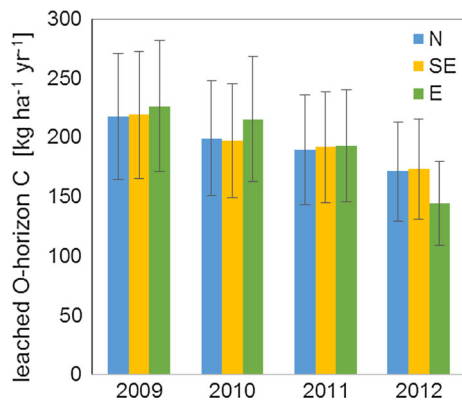
Spatial distribution of soil C fluxes

Given the strong relationships between water availability and C fluxes, we developed correlations between soil C parameters and hydrologic parameters (Fig. 4d) that we used to extrapolate C fluxes. For this we used the relationship between soil water and C fluxes established in E to estimate soil C fluxes using the regression equation for the correlation between dissolved soil C and soil water flux (see Fig. 4d). As water flux, we used model output for total precipitation because all water infiltrates at least into the shallow soil horizons (no overland flow, see online resource).

C leached from shallow soil horizons was dominated by DOC accounting for $87 \pm 13\%$ of total dissolved C (data not shown) and total C fluxes (DOC + DIC) ranged from ca. 140 to over 200 kg C ha^{-1} year^{-1} (Fig. 5). Overlapping error bars indicate that the differences between years (and catchments) are not significant, as was confirmed by repeated measures ANOVA (prob > F was 0.3 and 0.9 for difference between years and catchment,

Fig. 4 Selected correlation of water versus C fluxes. **a** effective summer precipitation (P$_{eff}$ summer between 06/01 and 09/30) versus ecosystem respiration (R), **b** maximum snow water equivalent (SWE$_{max}$) versus net ecosystem exchange (NEE), **c** Annual P$_{eff}$ versus total stream water C flux, **d** Soil water flux versus soil C (DOC and DIC) flux. Regression is shown for O-horizon samples only (for all depth excluding the wetland samples r^2 was 0.78, p < 0.0001). Note that negative NEE values signify net ecosystem uptake

Fig. 5 C leached from O-horizons calculated from total precipitation and the relationship between water and soil C fluxes from passive capillary wick samplers (PCAPS) in the headwaters of E

Table 6 Estimated C stored in each catchment as measured by: (1) above and belowground biomass C derived from the LiDAR mean canopy height (MCH); (2) median woody debris and duff C extrapolated by forest type and total area of each type, (3) herbaceous biomass extrapolated from average C by measured range monitoring transects and total area of each type

	N	SE	E
Area weighted biomass C density (Mg C ha^{-1})			
Mean	134 ± 40	230 ± 69	222 ± 67
Biomass C density by landscape position (Mg C ha^{-1})			
Hillslope C	123 ± 37	223 ± 67	219 ± 66
Riparian C	184 ± 55	275 ± 83	237 ± 71
Biomass C reservoir (Mg)			
1 forest C	41,749	52,450	82,066
2 debris + duff C	5362	4482	7201
3 herbaceous C	180	198	165
Total	47,291	57,130	89,432
Soil organic carbon (Mg C ha^{-1})			
Hillslope SOC	95 ± 24	76 ± 13	110 ± 35
Riparian SOC	204 ± 14	115 ± 8	208 ± 14
Weighted mean	114 ± 30	81 ± 15	125 ± 41

Average tons per hectare (Mg C ha^{-1}) extrapolated by (4) hillslope SOC, (5) riparian SOC, and (6) hillslope aboveground C (AGC), (7) riparian AGC weighted average per hectare values include non-forested areas, e.g. Felsenmeer fields, meadows and mountain grasslands. Error for biomass density was set to 30% since simple error propagation inflated the error due to the presence of few old growth stands with high biomass. Error for soil organic carbon (SOC) was propagated from error of C measurement and spatial distribution

respectively). Part of this C leached from shallow soil horizons was partitioned into shallow ground water, the volume and composition of which we estimated from water storage (Zapata Rios et al. 2015a, b) and spring water composition for two water years (2010 and 2011). Highest ground water storage volume was estimated for N in 2010 followed by E in 2010, whereas lowest storage volume was estimated for SE in both years (Table 5). Dissolved C in shallow ground water was dominated by DIC (accounting for up to 80% of dissolved C) and highest for E (Table 5) but did not exceed 6 kg C ha^{-1} year^{-1}, thus representing less than 4% of leached C.

Reservoirs: biomass and soil C

Total biomass C storage was lowest in N catchment (Table 6; Fig. 6a) with the difference due to percent forest cover, grassland, exposed rock, and, importantly, landscape position. Across all three catchments, above ground biomass was up to 1.5 times higher in riparian and convergent areas than on hillslope positions (Table 6). The total biomass C in each of the three catchments also varied greatly based on modern land use history with the lowest biomass for forest types recorded in the logged areas (Fig. 6c).

Based on the sampled soil profile data, the largest soil C stores were found in convergent zone soils, which contain up to twice as much C as planar or

Table 5 Groundwater dissolved organic and inorganic carbon (DIC and DOC) in kg ha^{-1} for three catchments and 2 years

	2010			2011		
	N	SE	E	N	SE	E
GW volume (m^3)	9E+04	2E+04	5E+04	3E+04	2E+04	4E+04
DOC	0.21	1.14	0.72	0.60	1.10	0.58
SD	0.28	0.60	0.56	0.47	0.59	0.50
DIC	1.54	1.86	5.11	4.34	1.79	4.10
SD	0.34	0.57	0.64	0.57	0.56	0.57
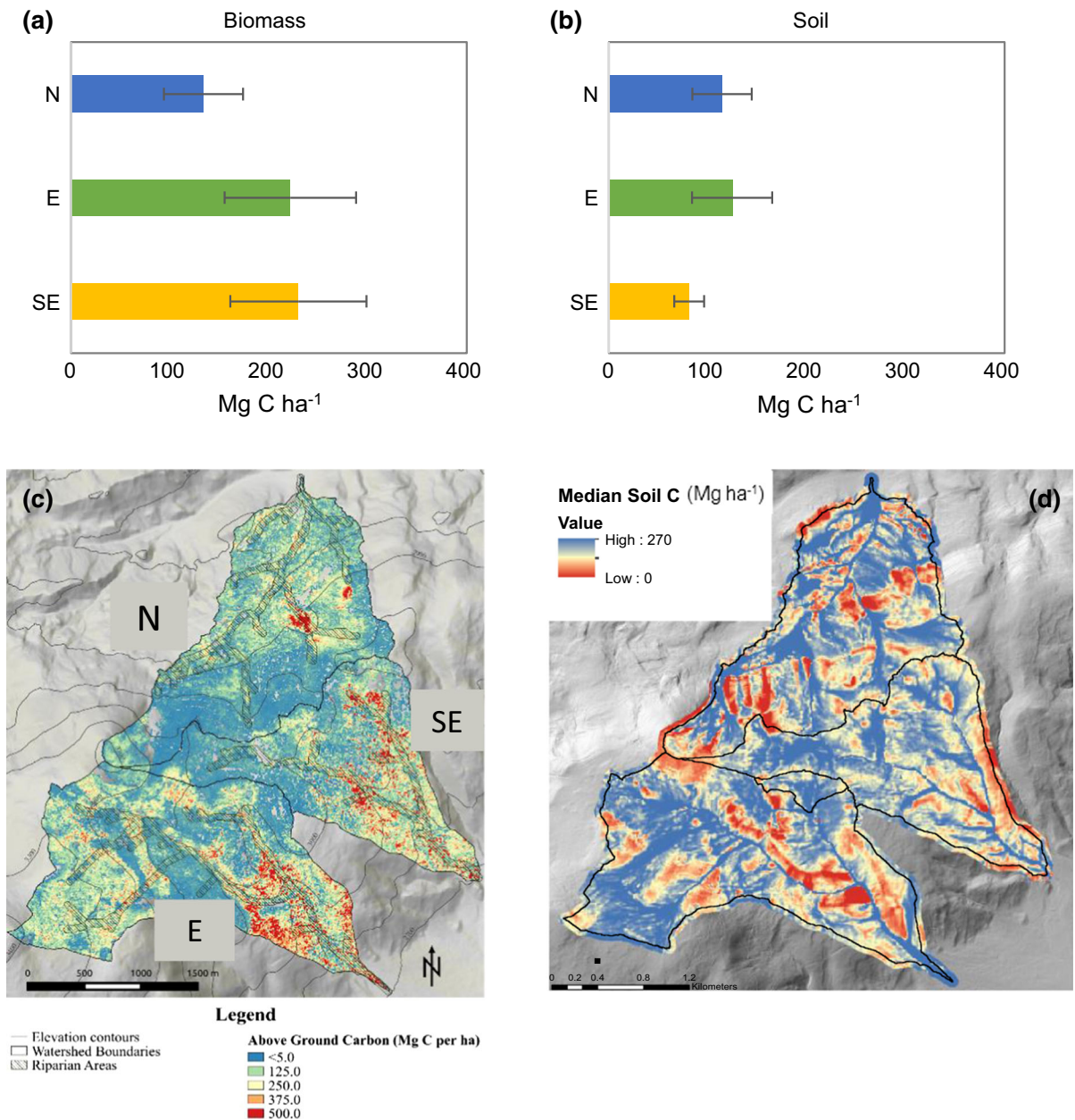
Fig. 6 a Above Ground Biomass C (AGB) and **b** total soil C stocks, representing the sum of average mineral horizon C stocks and average organic horizon C stocks. Simple error propagation of mineral and organic horizon C stock standard deviations was used to constrain the error on total soil C stock estimates. **c** spatial distribution of AGB and **d** soil C based on soil depth

divergent hillslopes in the same catchment (N and E, Table 6). N and E show similar amounts of SOC while SE stores 20-30% less C in hillslope positions and 40% less in convergent zones than E and N. The weighted average SOC content based on the relative contribution of convergent versus non-convergent

landscape positions shows a similar trend: overall E stores the most SOC, followed by N while SE exhibits the smallest SOC stores (Fig. 6b). Spatial estimates of soil C stocks followed landscape patterns of topographic variation, with the largest C stores in

convergent areas and relatively low sloping hillslopes and uplands with deep soils (Fig. 6d).

To test whether we can scale the observation of links between catchment wetness and soil C stores down to wet versus dry landscape positions within each catchment, we compared modeled SOC distribution (which includes, by way of model calculation, consideration of landscape-position dependent soil depth) with topographic wetness index (TWI), radiation, and EEMT (see Fig. 2). Results indicate that the best predictor of C is TWI, explaining > 50% of C variance, with strong positive correlation (i.e., wet locations have high C).

Discussion

Our results suggest that seasonal differences in precipitation influence forest C storage through three mechanisms. First, winter precipitation is a primary control on C uptake during the next growing season, while summer precipitation stimulates respiration to a greater extent than photosynthesis. Second, lateral redistribution of soil solution and ground water result in large above-ground biomass stores in riparian and convergent zones relative to upslope or flat topographic positions. Third, the same dynamics lead to large soil C stores in riparian and convergent zones relative to upslope or flat topographic positions. We discuss each of these findings in more detail below, including implications for suggested changes in the seasonality of precipitation that may influence forest C storage under a changing climate.

Timing of water availability controls C fluxes in the CZ

We had hypothesized that timing of water availability controls C fluxes through differentially influencing the balance of photosynthesis and respiration. Specifically we hypothesized that GPP would be highest in years with wet winters because deep rooted, autotrophic C fixation uses ground water that is recharged during snowmelt. Conversely, heterotrophic soil microorganisms access water in shallow soil horizons, and are most active in warm, wet soils. We therefore had hypothesized that ecosystem respiration (R) is greatest in years with wet summers. As a result, net ecosystem

exchange (NEE) was postulated to be smallest in years with dry winters and wet summers.

We indeed found that summer versus winter precipitation differentially impacted C dynamics: winter snow increased net ecosystem C uptake, and both GPP and NEE correlated strongly (positively and negatively, respectively) with maximum SWE (Fig. 4b). Snowmelt represents a large water input into our systems and is mostly partitioned into ground water recharge (Zapata-Rios et al. 2015a), whereas summer convective storms deliver relatively small pulses of repeated precipitation to our catchments. These pulses are lost quickly to evaporation and transpiration following shallow root uptake, yielding little deep infiltration. Therefore autotrophs may be water-limited even during the relatively wet monsoon season if no deeper water source is available, leading to decreased productivity and overall decline in net C uptake (Hu et al. 2010).

We also found that summer rains increased ecosystem respiration (Fig. 4a). Wetting of warm organic-rich soil horizons stimulates heterotrophic C processing, increasing ecosystem respiration, which is confirmed by the positive correlation between respiration and summer precipitation (and a positive correlation between effective summer precipitation and NEE indicating decreased C uptake with increased summer rains). These results are in agreement with a growing body of work that suggests that increases in soil moisture and warmer temperatures during summer favor soil respiration and can offset plant C uptake (Huxman et al. 2004a; Potts et al. 2006; Stielstra et al. 2015).

While these results are in agreement with our hypotheses, they diverge from other studies because of system-level variation in factors limiting C uptake. For example, Öquist et al. (2014) found that increased precipitation *decreased* net C uptake in a boreal forest because of decreased radiant energy inputs. Additionally, a reduction in winter snow cover in northeastern hardwood forests *increased* net C uptake because of longer growing season (Groffman et al. 2012). These examples highlight that catchment-scale C budgets are strongly impacted by complex interactions between amount and timing of delivery of a productivity-limiting component such as energy or water. They also reveal that the nature and identity of limiting components vary with the system of study.

Table 7 Carbon effluxes and internal fluxes represented as % of NEE for all catchments (*O* organic, *GW* ground water)

	N				SE				E			
	2009	2010	2011	2012	2009	2010	2011	2012	2009	2010	2011	2012
Stream water (dissolved)												
		0.25	0.12	0.15		0.16	0.05	0.08		0.15	0.07	0.08
Leached from O horizons												
	4.2	3.2	4.6	2.6	4.2	3.2	4.7	2.6	4.4	3.5	4.7	2.2
Shallow GW												
		0.3	0.4			0.5	0.7			0.9	1.4	

Because snowmelt is mostly partitioned into ground water and summer rain promotes soil respiration and evapotranspiration, we had hypothesized that aqueous C fluxes (soil and steam water) would be small. Indeed, stream water C effluxes were very small relative to vertical ecosystem fluxes and, on average, accounted for less than 0.3% of annual NEE (Table 7). Proportionately higher values (up to 11%) have been reported for non-water limited, forested systems (Brunet et al. 2009; Jonsson et al. 2007; Öquist et al. 2014; Shibata et al. 2005; Zhou et al. 2013). Most stream water C in our catchments was exported as an annual pulse during snowmelt, consistent with the flushing of DOC from soils (Boyer et al. 1997, 2000; Huxman et al. 2004b; Perdrial et al. 2014a; Sanderman et al. 2009), and correlated with effective precipitation (Fig. 4c).

Soil water C fluxes are also small but larger than stream water fluxes. Soil solutions show significantly higher C fluxes through O horizons than through A or B/C horizons (Fig. 3), indicating significant transfer. Vertical transfer and interception of this C in deeper horizons is not observed (Vázquez-Ortega et al. 2015), and soil CO_2 effluxes during snowmelt, when soil water flux is highest, are relatively low [2–4 times lower than during summer months (Stielstra et al. 2015)]. We therefore conclude that, similar to N (Biederman et al. 2016; Weintraub et al. 2017), a large fraction of dissolved soil C is transported laterally to convergent landscape positions during snowmelt (Fig. 5), accounting for 2–5% of NEE, and representing the largest aqueous flux in our systems (Table 7). Lateral C transfer to convergent zones has been postulated previously (Bourgault et al. 2017; Lv et al. 2013) and our findings of substantially larger C stores

in riparian soils versus hillslope locations (Table 6, Fig. 6d) are in agreement with the concept of landscape position as driver of soil C (Bailey et al. 2014; Conforti et al. 2016; Holleran et al. 2015; Lybrand and Rasmussen 2015).

Long-term trends in catchment wetness control C stores

We hypothesized that long-term trends in C uptake would be reflected in the magnitude of biomass and soil C stores, and that the wettest catchments would exhibit largest stores (hypothesis 3). Our study catchments are located in close proximity to each other and share many characteristics, but differ in water inputs and hydrologic partitioning (Table 3), enabling a direct test of this hypothesis. Of the three catchments, E, is the wettest with highest maximum SWE, and total and effective precipitation. In this specific case wetness is impacted by topographic shading from the adjacent Redondito dome (Fig. 1a), which limits evaporation and sublimation, providing conditions that are more typically associated with N aspects. In contrast, the adjacent SE received the least amount of precipitation for most years and is driest (Table 3).

Because we found that winter precipitation drives ecosystem C uptake and summer rains enhance C losses, it is reasonable to predict that catchments with higher winter to summer precipitation ratio (E, followed by N) should exhibit the greatest stores. For biomass, however, both E and SE exhibit similarly high above ground biomass while lowest biomass C was found for N (Fig. 6). One possible explanation for the lower biomass in N could be energy (rather than water) limitation since N receives significantly less

solar radiation (even taking topographic shading of E into account, Fig. 2a)—a contention that is supported by findings by Anderson-Teixeira et al. (2011) and Zapata-Rios et al. (2015b). Another complicating factor is spatially patchy logging 50–100 years ago, where N was logged more intensively.

Although soil stores are also impacted by logging (Bradford et al. 2012; Chen and Shrestha 2012), they are better suited to test our hypothesis on the link between wetness, net C uptake and C storage, because the logging effect on SOC is expected to be smaller. Indeed, the magnitude of soil stores (ca. 120 Mg C ha^{-1}) is in the range of estimates for similar systems (50–200 Mg C ha^{-1}) (Dahlgren et al. 1997; Heckman and Rasmussen 2011; Rasmussen et al. 2007)). As hypothesized, greatest soil C stores were found in E and lowest in SE (Table 6, Fig. 6a, b). Higher wetness promotes enhanced productivity, leading to increased leaf litter production, root exudation, and biomass turnover, thereby increasing soil C.

From sink to source: insights from a combined water and net ecosystem C balance

The quantification of gaseous and dissolved C fluxes revealed that all fluxes (lateral and vertical) are driven by the timing, form and amount of precipitation. Since net ecosystem C uptake and storage results from the balance of competing transport and fate pathways, impacts of climate variation are paramount. In the present case net C uptake responded positively to snow-derived water but not to growing season precipitation. As a result of high net C uptake, the studied catchments were a substantive sink for C during throughout study period (Table 4). Our (negative) NEE values suggest accumulation of substantial stores in biomass and soils that potentially reflect trends in catchment water (and possibly energy) delivery. However, we note that (i) magnitude of NEE values reported here may be overestimated because flux towers in ridge top locations can underestimate respiration, especially CO_2 losses via lateral advection and cold-air drainage of nighttime respiration (Pypker et al. 2007) and (ii) these ca. 70 year old forests are likely at the peak of their productivity and GPP will decrease with stand age (Amiro et al. 2010). Therefore, we cannot conclude unequivocally that this forested CZ represents a C sink with long-term persistence. To the contrary, the data presented here

suggest that a transition from winter snow to summer rain dominance could decrease deep water infiltration, thereby decreasing GPP and promoting ecosystem respiration, hence lowering overall net C uptake.

References

Allen CD (1989) Changes in the landscape of the Jemez Mountains, vol 346. UC Berkley, New Mexico

Amiro BD, Barr AG, Barr JG, Black TA, Bracho R, Brown M, Chen J, Clark KL, Davis KJ, Desai AR, Dore S, Engel V, Fuentes JD, Goldstein AH, Goulden ML, Kolb TE, Lavigne MB, Law BE, Margolis HA, Martin T, McCaughey JH, Misson L, Montes-Helu M, Noormets A, Randerson JT, Starr G, Xiao J (2010) Ecosystem carbon dioxide fluxes after disturbance in forests of North America. J Geophys Res 115(G4):G00K02

Anderson-Teixeira KJ, Delong JP, Fox AM, Brese DA, Litvak ME (2011) Differential responses of production and respiration to temperature and moisture drive the carbon balance across a climatic gradient in New Mexico. Glob Change Biol 17(1):410–424

Bailey SW, Brousseau PA, McGuire KJ, Ross DS (2014) Influence of landscape position and transient water table on soil development and carbon distribution in a steep, headwater catchment. Geoderma 226–227:279–289

Battin TJ, Luyssaert S, Kaplan LA, Aufdenkampe AK, Richter A, Tranvik LJ (2009) The boundless carbon cycle. Nat Geosci 2(9):598–600

Beven K, Kirkby MJ (1979) A physically based, variable contributing area model of basin hydrology/Un modèle à base physique de zone d'appel variable de l'hydrologie du bassin versant. Hydrol Sci J 24(1):43–69

Biederman JA, Meixner T, Harpold AA, Reed DE, Gutmann ED, Gaun JA, Brooks PD (2016) Riparian zones attenuate nitrogen loss following bark beetle-induced lodgepole pine mortality. J Geophys Res 121(3):933–948

Bloom AA, Exbrayat J-F, van der Velde IR, Liang F, Williams M (2016) The decadal state of the terrestrial carbon cycle: global retrievals of terrestrial carbon allocation, pools, and residence times. Proc Natl Acad Sci USA 113(5):1285–1290

Bourgault RR, Ross DS, Bailey SW, Bullen TD, McGuire KJ, Gannon JP (2017) Redistribution of soil metals and organic carbon via lateral flowpaths at the catchment scale in a glaciated upland setting. Geoderma 307:238–252

Boyer EW, Hornberger GM, Bencala KE, McKnight DM (1997) Response characteristics of DOC flushing in an alpine catchment. Hydrol Process 11(12):1635–1647

Boyer EW, Hornberger GM, Bencala KE, McKnight DM (2000) Effects of asynchronous snowmelt on flushing of dissolved organic carbon: a mixing model approach. Hydrol Process 14(18):3291–3308

Bradford MA, Crowther TW (2013) Carbon use efficiency and storage in terrestrial ecosystems. New Phytol 199(1):7–9

Bradford JB, Fraver S, Milo AM, Damato AW, Palik B, Shinneman DJ (2012) Effects of multiple interacting disturbances and salvage logging on forest carbon stocks. For Ecol Manag 267:209–214

Breshears DD, Huxman TE, Adams HD, Zou CB, Davison JE (2008) Vegetation synchronously leans upslope as climate warms. Proc Natl Acad Sci USA 105(33):11591–11592

Brooks PD, Vivoni ER (2008) Mountain ecohydrology: quantifying the role of vegetation in the water balance of montane catchments. Ecohydrology 1(3):187–192

Brown J (1971) A planar intersect method for sampling fuel volume and surface area. For Sci 17(1):96–102

Broxton PD, Troch PA, Lyon SW (2009) On the role of aspect to quantify water transit times in small mountainous catchments. Water Resour Res 45(8):W08427

Broxton PD, Harpold AA, Biederman JA, Troch PA, Molotch NP, Brooks PD (2015) Quantifying the effects of vegetation structure on snow accumulation and ablation in mixedconifer forests. Ecohydrology 8(6):1073–1094

Brunet F, Dubois K, Veizer J, Nkoue Ndondo GR, Ndam Ngoupayou JR, Boeglin JL, Probst JL (2009) Terrestrial and fluvial carbon fluxes in a tropical watershed: Nyong basin, Cameroon. Chem Geol 265(3–4):563–572

Cairns MA, Brown S, Helmer EH, Baumgardner GA (1997) Root biomass allocation in the world's upland forests. Oecologia 111(1):1–11

Chen HYH, Shrestha BM (2012) Stand age, fire and clearcutting affect soil organic carbon and aggregation of mineral soils in boreal forests. Soil Biol Biochem 50:149–157

Ciais P, Reichstein M, Viovy N, Granier A, Ogée J (2005) Europe-wide reduction in primary productivity caused by the heat and drought in 2003. Nat 437:529–533

Conforti M, Lucà F, Scarciglia F, Matteucci G, Buttafuoco G (2016) Soil carbon stock in relation to soil properties and landscape position in a forest ecosystem of southern Italy (Calabria region). CATENA 144:23–33

Coop JD, Givnish TJ (2007) Spatial and temporal patterns of recent forest encroachment in montane grasslands of the Valles Caldera, New Mexico, USA. J Biogeogr 34(5):914–927

Dahlgren RA, Boettinger JL, Huntington GL, Amundson RG (1997) Soil development along an elevational transect in the western Sierra Nevada, California. Geoderma 78(3–4):207–236

Efron B, Stein C (1981) The Jackknife estimate of variance. Ann Stat 9(3):586–596

Fan Y, Li H, Miguez-Macho G (2013) Global patterns of groundwater table depth. Science 339(6122):940–943

Fu P, Rich PM (1999) Design and implementation of the solar analyst: an arc view extension for modeling solar radiation at landscape scales. Proc Nineteenth Annu ESRI User Conf 1:1–31

Gochis DJ, Vivoni ER, Watts CJ (2010) The impact of soil depth on land surface energy and water fluxes in the North American Monsoon region. J Arid Environ 74(5):564–571

Groffman PM, Rustad LE, Templer PH, Campbell JL, Christenson LM, Lany NK, Socci AM, Vadeboncoeur MA, Schaberg PG, Wilson GF, Driscoll CT, Fahey TJ, Fisk MC, Goodale CL, Green MB, Hamburg SP, Johnson CE, Mitchell MJ, Morse JL, Pardo LH, Rodenhouse NL (2012) Long-term integrated studies show complex and surprising effects of climate change in the Northern hardwood forest. Bioscience 62(12):1056–1066

Heckman K, Rasmussen C (2011) Lithologic controls on regolith weathering and mass flux in forested ecosystems of the southwestern USA. Geoderma 164(3–4):99–111

Heckman K, Welty-Bernard A, Rasmussen C, Schwartz E (2009) Geologic controls of soil carbon cycling and microbial dynamics in temperate conifer forests. Chem Geol 267(1–2):12–23

Holleran M, Levi M, Rasmussen C (2015) Quantifying soil and critical zone variability in a forested catchment through digital soil mapping. Soil 1(1):47–64

Houghton RA (2005) Aboveground forest biomass and the global carbon balance. Glob Change Biol 11:945

Houghton RA (2007) Balancing the global carbon budget. Annu Rev Earth Planet Sci 35(1):313–347

Houghton RA, Davidson EA, Woodwell GM (1998) Missing sinks, feedbacks, and understanding the role of terrestrial ecosystems in the global carbon balance. Glob Biogeochem Cycles 12(1):25–34

Hu JIA, Moore DJP, Burns SP, Monson RK (2010) Longer growing seasons lead to less carbon sequestration by a subalpine forest. Glob Change Biol 16(2):771–783

Huxman T, Cable J, Ignace D, Eilts JA, English N, Weltzin J, Williams D (2004a) Response of net ecosystem gas exchange to a simulated precipitation pulse in a semi-arid grassland: the role of native versus non-native grasses and soil texture. Oecologia 141(2):295–305

Huxman TE, Snyder KA, Tissue D, Leffler AJ, Ogle K, Pockman WT, Sandquist DR, Potts DL, Schwinning S (2004b) Precipitation pulses and carbon fluxes in semiarid and arid ecosystems. Oecologia 141(2):254–268

IPCC (2013) The physical science basis. In: Stocker TF, Qin D, Plattner G-K, Tignor M, Allen SK, Boschung J, Nauels A, Xia Y, Bex V, Midgley PM (eds) Contribution of Working Group 1 to the Fifth Assessment Report of the Intergovernmental Panel on Climate Change. Cambridge University Press, Cambridge, United Kingdom and New York, NY, USA, p 1535

Jackson RB, Canadell J, Ehleringer JR, Mooney HA, Sala OE, Schulze ED (1996) A global analysis of root distributions for terrestrial biomes. Oecologia 108(3):389–411

Jonsson A, Algesten G, Bergström AK, Bishop K, Sobek S, Tranvik LJ, Jansson M (2007) Integrating aquatic carbon fluxes in a boreal catchment carbon budget. J Hydrol 334(1–2):141–150

Kaiser K, Guggenberger G, Zech W (1996) Sorption of DOM and DOM fractions to forest soils. Geoderma 74(3–4):281–303

Keith H, Mackey BG, Lindenmayer DB (2009) Re-evaluation of forest biomass carbon stocks and lessons from the world's most carbon-dense forests. Proc Natl Acad Sci USA 106(28):11635–11640

Lal R (2004) Soil carbon sequestration impacts on global climate change and food security. Science 304(5677):1623–1627

Lal R (2005) Forest soils and carbon sequestration. For Ecol Manag 220(1–3):242–258

Litton CM, Raich JW, Ryan MG (2007) Carbon allocation in forest ecosystems. Glob Change Biol 13(10):2089–2109

Liu F, Parmenter R, Brooks PD, Conklin MH, Bales RC (2008) Seasonal and interannual variation of streamflow pathways and biogeochemical implications in semi-arid, forested catchments in Valles Caldera, New Mexico. Ecohydrology 1(3):239–252

Lv M, Hao Z, Liu Z, Yu Z (2013) Conditions for lateral downslope unsaturated flow and effects of slope angle on soil moisture movement. J Hydrol 486:321–333

Lybrand RA, Rasmussen C (2015) Quantifying climate and landscape position controls on soil development in semi-arid ecosystems. Soil Sci Soc Am J 79(1):104–116

Mahat V, Tarboton DG (2012) Canopy radiation transmission for an energy balance snowmelt model. Water Resour Res 48(1):W01534

Muldavin E, Tonne P (2003) A vegetation survey and preliminary ecological assessment of valles Caldera National preserve, New Mexico. Natural Heritage, Albuquerque

Muldavin E, Tonne P, Jackson C (2006) A vegetation map of the Valles Caldera National Preserve, New Mexico. In: Final Report for Cooperative Agreement, vol 01CRAG0014

Öquist MG, Bishop K, Grelle A, Klemedtsson L, Köhler SJ, Laudon H, Lindroth A, Ottosson Löfvenius M, Wallin MB, Nilsson MB (2014) The full annual carbon balance of boreal forests is highly sensitive to precipitation. Environ Sci Technol Lett 1(7):315–319

Park Williams A, Allen CD, Macalady AK, Griffin D, Woodhouse CA, Meko DM, Swetnam TW, Rauscher SA, Seager R, Grissino-Mayer HD, Dean JS, Cook ER, Gangodagamage C, Cai M, McDowell NG (2013) Temperature as a potent driver of regional forest drought stress and tree mortality. Nat Clim Change 3(3):292–297

Parmentier RR, Steffen A, Allen C (2007) An overview of the Valles Caldera National Preserve: The natural and cultural resources. In: Kues BS, Kelley, Shari A, Lueth, Virgil W (ed) New Mexico Geological Society 58th Annual Fall Field Conference

Pelletier JD, Rasmussen C (2009) Geomorphically based predictive mapping of soil thickness in upland watersheds. Water Resour Res Banner 45(9). https://doi.org/10.1029/2008WR007319

Perdrial JN, Perdrial N, Harpold A, Gao X, LaSharr KM, Chorover J (2012) Impacts of sampling dissolved organic matter with passive capillary wicks versus aqueous soil extraction. Soil Sci Soc Am J 76:2019–2030

Perdrial JN, McIntosh JC, Harpold A, Brooks PD, Zapata-Rios X, Ray J, Meixner T, Kanduc T, Litvak M, Troch P, Chorover J (2014a) Stream water carbon controls in seasonally snow-covered mountain catchments: impact of inter annual variability of water fluxes, catchment aspect and seasonal processes. Biogeochemistry 118(1–3):273–290

Perdrial JN, Perdrial N, Vazquez-Ortega A, Porter CM, Leedy J, Chorover J (2014b) Experimental assessment of fiberglass passive capillary wick sampler (PCap) suitability for sampling inorganic soil solution constituents. Soil Sci Soc Am J 78:486–495

Pomeroy JW, Parviainen J, Hedstrom N, Gray DM (1998) Coupled modelling of forest snow interception and sublimation. Hydrol Process 12(15):2317–2337

Potts DL, Huxman TE, Cable JM, English NB, Ignace DD, Eilts JA, Mason MJ, Weltzin JF, Williams DG (2006) Antecedent moisture and seasonal precipitation influence the response of canopy-scale carbon and water exchange to rainfall pulses in a semi-arid grassland. New Phytol 170(4):849–860

Pypker TG, Unsworth MH, Lamb B, Allwine E, Edburg S, Sulzman E, Mix AC, Bond BJ (2007) Cold air drainage in a forested valley: investigating the feasibility of monitoring ecosystem metabolism. Agric For Meteorol 145(3):149–166

Rasmussen C, Matsuyama N, Dahlgren RA, Southard RJ, Brauer N (2007) Soil genesis and mineral transformation across an environmental gradient on andesitic Lahar. Soil Sci Soc Am J 71(1):225–237

Rasmussen C, Troch P, Chorover J, Brooks P, Pelletier J, Huxman T (2011) An open system framework for integrating critical zone structure and function. Biogeochemistry 102(1–3):15–29

Rasmussen C, Pelletier JD, Troch PA, Swetnam TL, Chorover J (2015) Quantifying topographic and vegetation effects on the transfer of energy and mass to the critical zone. Vadose Zone J 14(11):1–16

Robinson D (2004) Scaling the depths: below-ground allocation in plants, forests and biomes. Funct Ecol 18(2):290–295

Rowson JG, Gibson HS, Worrall F, Ostle N, Burt TP, Adamson JK (2010) The complete carbon budget of a drained peat catchment. Soil Use Manag 26(3):261–273

Sanderman J, Lohse KA, Baldock JA, Amundson R (2009) Linking soils and streams: sources and chemistry of dissolved organic matter in a small coastal watershed. Water Resour Res 45(3):W03418

Santantonio D, Hermann RK (1985) Standing crop, production, and turnover of fine-roots on dry, moderate and wet sites of mature Douglas-fir in western Oregon. Ann For Sci 42:113–142

Schimel DS, House JI, Hibbard KA, Bousquet P, Ciais P, Peylin P, Braswell BH, Apps MJ, Baker D, Bondeau A, Canadell J, Churkina G, Cramer W, Denning AS, Field CB, Friedlingstein P, Goodale C, Heimann M, Houghton RA, Melillo JM, Moore B, Murdiyarso D, Noble I, Pacala SW, Prentice IC, Raupach MR, Rayner PJ, Scholes RJ, Steffen WL, Wirth C (2001) Recent patterns and mechanisms of carbon exchange by terrestrial ecosystems. Nature 414(6860):169–172

Schmidt MW, Torn MS, Abiven S, Dittmar T, Guggenberger G, Janssens IA, Kleber M, Kogel-Knabner I, Lehmann J, Manning DA, Nannipieri P, Rasse DP, Weiner S,

Trumbore SE (2011) Persistence of soil organic matter as an ecosystem property. Nature 478(7367):49–56

Shibata H, Hiura T, Tanaka Y, Takagi K, Koike T (2005) Carbon cycling and budget in a forested basin of southwestern Hokkaido, northern Japan. In: Kohyama T, Canadell J, Ojima D, Pitelka L (eds) Forest ecosystems and environments. Springer, Tokyo, pp 89–95

SoilSurveyStaff (2011) Keys to soil taxonomy. In: United States Department of Agriculture NRCS, p 339

Stielstra C, Brooks PD, Lohse KA, McIntosh JM, Chorover J, Barron-Gafford G, Perdrial JN, Barnard HR, Litvak M (2015) Climatic and landscape influences on soil moisture are primary determinants of soil carbon fluxes in seasonally snow-covered forest ecosystems. Biogeochemistry 123:447–465

Swetnam TL (2013) Cordilleran forest scaling dynamics and disturbance regimes quantified by aerial LiDAR. In: School of natural resources. University of Arizona

Tarboton DG, Bras RL, Rodriguez-Iturbe I (1991) On the extraction of channel networks from digital elevation data. Hydrol Process 5(1):81–100

Thompson SE, Harman CJ, Konings AG, Sivapalan M, Neal A, Troch PA (2011a) Comparative hydrology across Ameri-Flux sites: the variable roles of climate, vegetation, and groundwater. Water Resour Res. https://doi.org/10.1029/2010WR009797.W00J07

Thompson SE, Harman CJ, Troch PA, Brooks PD, Sivapalan M (2011b) Spatial scale dependence of ecohydrologically mediated water balance partitioning: a synthesis framework for catchment ecohydrology. Water Resour Res. https://doi.org/10.1029/2011WR011377

Torn MS, Trumbore SE, Chadwick OA, Vitousek PM, Hendricks DM (1997) Mineral control of soil organic carbon storage and turnover. Nature 389(6647):170–173

USFS In: Report SEC (ed). Valles caldera trust, Valles caldera national perserve, p 11. (**unpublished data**)

Vazquez-Ortega A (2013) Coupled transport, fractionation and stabilization of dissolved organic matter and rare earth elements in the critical zone. In: Department of Soil Water and Environmental Sciences, University of Arizona, Tucson

Vázquez-Ortega A, Perdrial JN, Harpold A, Zapata X, Rasmussen C, McIntosh J, Schaap M, Pelletier J, Brooks P, Amistadi MK, Chorover J (2015) Rare earth elements as reactive tracers of biogeochemical weathering in forested rhyolitic terrain. Chem Geol 391:19–32

Weintraub SR, Brooks PD, Bowen GJ (2017) Interactive effects of vegetation type and topographic position on nitrogen availability and loss in a temperate montane ecosystem. Ecosystems 20(6):1073–1088

Whittaker RH, Niering WA (1975) Vegetation of the Santa Catalina Mountains, Arizona. V. Biomass, production, and diversity along the elevation gradient. Ecology 56(4):771–790

Winstral A, Elder K, Davis RE (2002) Spatial snow modeling of wind-redistributed snow using terrain-based parameters. J Hydrometeorol 3(5):524–538

Zapata-Rios X, Troch PA, McIntosh J, Broxton P, Harpold AA, Brooks PD (2012) When winter changes: differences in the hydrological response from first-order catchments of similar age in New Mexico. In: American Geophysical Union Fall Meeting, San Francisco

Zapata-Rios X, McIntosh J, Rademacher L, Troch PA, Brooks PD, Rasmussen C, Chorover J (2015a) Climatic and landscape controls on water transit times and silicate mineral weathering in the critical zone. Water Resour Res 51(8):6036–6051

Zapata-Rios X, Brooks PD, Troch PA, McIntosh J, Guo Q (2015b) Influence of terrain aspect on water partitioning, vegetation structure, and vegetation greening in high elevation catchments in northern New Mexico. Ecohydrology 9(5):782–795

Zhou W-J, Zhang Y-P, Schaefer DA, Sha L-Q, Deng Y, Deng X-B, Dai K-J (2013) The role of stream water carbon dynamics and export in the carbon balance of a tropical seasonal rainforest, Southwest China. PLoS ONE 8(2):e56646